

Hall effect and two-dimensional electron gas in black phosphorus

This article has been downloaded from IOPscience. Please scroll down to see the full text article.

1992 J. Phys.: Condens. Matter 4 1535

(<http://iopscience.iop.org/0953-8984/4/6/018>)

View [the table of contents for this issue](#), or go to the [journal homepage](#) for more

Download details:

IP Address: 171.66.16.159

The article was downloaded on 12/05/2010 at 11:16

Please note that [terms and conditions apply](#).

Hall effect and two-dimensional electron gas in black phosphorus

M Baba[†], Y Nakamura[†], Y Takeda[†], K Shibata[‡], A Morita[§], Y Koike^{||}
and T Fukase[¶]

[†] Department of Electronic Engineering, Iwate University, Morioka 020, Japan

[‡] Aomori Polytechnic College, Goshogawara 037, Japan

[§] Department of Basic Science, Ishinomaki Senshu University, Ishinomaki 986, Japan

^{||} Department of Applied Physics, Tohoku University, Sendai 980, Japan

[¶] Institute for Materials Research, Tohoku University, Sendai 980, Japan

Received 23 May 1991, in final form 1 October 1991

Abstract. The Hall coefficient and electric conductivity of black phosphorus prepared by the bismuth-flux method were measured at low temperatures. It is found that the conductivity shows $\log T$ -like behaviour below about 5 K and the Hall coefficient changes its sign from plus to minus at around 7 K with decreasing temperature. These results can be analysed successfully on the basis of a three-carrier model, in which bulk holes, variable-range-hopping holes and two-dimensional electrons take part in the electric conduction at low temperatures, except in the case of strong magnetic fields below 7 K. The present analysis supports the fact that magneto-electric properties observed at low temperatures in black phosphorus crystals originate from the 2D Anderson localization in an inversion layer on the surface.

1. Introduction

Black phosphorus (black P) is the most stable form of many allotropic modifications of elementary phosphorus. Until recently, measurements have been performed on the electrical transport properties of black P at low temperatures [1–4]. Recently, an interesting preliminary investigation of the two-dimensional (2D) Anderson-localization-like phenomena in a needle-like black P crystal has been reported by Iwasaki *et al* [5]. To study such phenomena in more detail we have made a detailed measurement and analysis of the negative magnetoresistance and argued that the phenomena can in fact be explained by the 2D Anderson localization theory [6]. We have also argued, based on the measurement of the Hall coefficient, that the 2D localization originates from an inversion layer on the surface [7].

The purpose of the present paper is to make a quantitative analysis of the Hall coefficient and the conductivity of black P at low temperatures in terms of a three-carrier model and herewith to give further support to the 2D Anderson localization in the inversion layer of black P.

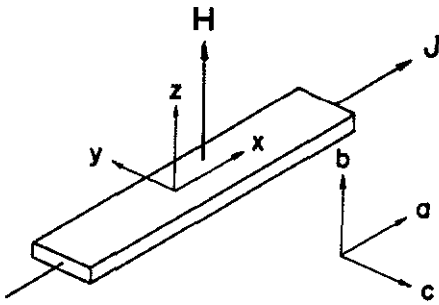


Figure 1. Geometry of a black-P sample used in the experiment, with an applied magnetic field (z axis), a current (x axis) and Hall contacts (y axis) for Hall measurements. The crystallographic axes a , b and c are also shown.

2. Experimental procedures

Single crystals of black P were prepared by the bismuth-flux method [8]. The prepared crystals are needle like and have a flat surface of the a - c plane. The size of the samples was typically 4 mm in length in the a axis direction, $100\ \mu\text{m}$ in width along the c axis, and $10\ \mu\text{m}$ in thickness along the b axis.

Figure 1 shows a schematic diagram of the geometry of a black-P sample used in the experiment. The electric field E is applied along the x axis and the magnetic field H is applied along the z axis. Resistance measurement was performed by the standard four-probe method with a constant current of $0.1\ \mu\text{A}$. The potential difference between potential probes was measured with a precision digital meter (Yokogawa Electric Works Ltd, type 2501). Gold paste was used to make the electric contacts between a sample and Au wires of $50\ \mu\text{m}$ diameter. In the Hall measurement, magnetic fields up to 15 kG were applied by a rotatable electric magnet. The Hall voltage was amplified with a microvolt meter (Ohkura Electric Co., model AM-1001) with a high input impedance and measured by the precision digital meter type 2501. The sample temperatures were measured with a Ge thermometer below 30 K and a Pt thermometer above 30 K.

3. Experimental results

From the previous experiments on the transport phenomena [7], we found that the black-P crystals exhibit p-type conduction associated with two species of acceptor. Their activation energies are 26.1 meV and 11.8 meV and the effective concentrations are typically $1.36 \times 10^{21}\ \text{m}^{-3}$ for the shallower level and $0.44 \times 10^{21}\ \text{m}^{-3}$ for the deeper level. The Hall mobility is given by the expression $\mu_H = 3.2 \times 10^2 T^{-3/2}\ \text{m}^2\ \text{V}^{-1}\ \text{s}^{-1}$ with the maximum value of $3.6\ \text{m}^2\ \text{V}^{-1}\ \text{s}^{-1}$ at around $T = 20\ \text{K}$.

Figure 2 shows the electric conductivity in the needle (a axis) direction for one of our samples as a function of temperature in the region $T < 30\ \text{K}$. An abrupt rise in conductivity above $T = 20\ \text{K}$ is ascribed to the conduction due to the holes activated from acceptors. On the other hand, the conductivity below 5 K shows a $\log T$ -like behaviour, which may be interpreted in terms of a different type of conduction associated with the two-dimensional Anderson localization [9].

The Hall measurement was performed for the same sample as that used in the electric conductivity measurement (figure 2). The observed Hall voltage was found to be proportional to the magnetic field above about 60 K as shown later in the inset in figure 4, while it was not below this temperature except in the case of the weak field. Figure 3

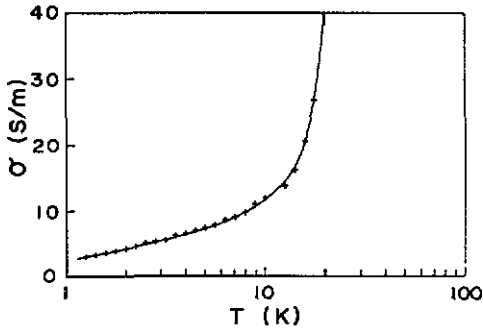


Figure 2. Electrical conductivity of black P observed in the low-temperature region.

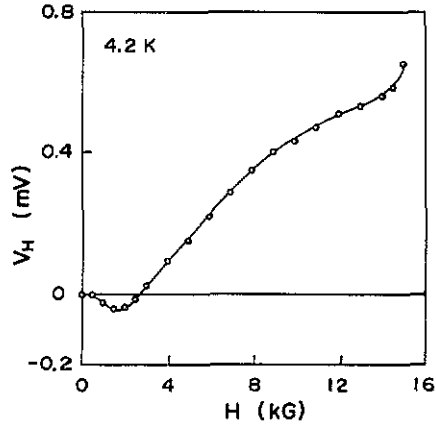


Figure 3. Observed Hall voltage as a function of magnetic field at 4.2 K.

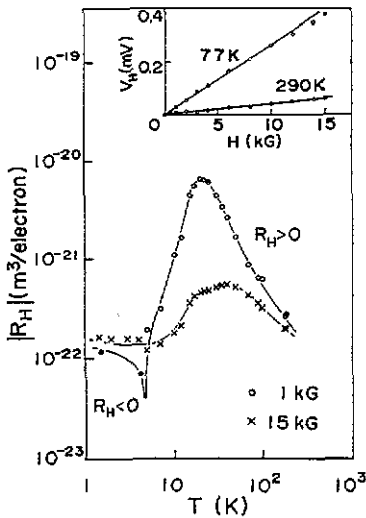


Figure 4. Observed Hall coefficients as a function of temperature at 1 kG (○) and 15 kG (×); —, guidelines for the eye; ●, R_H -values which are negative. The inset shows the linear dependence of the Hall voltage on the applied field at 77 and 290 K [7].

shows the magnetic field dependence of the Hall voltage measured at 4.2 K. The Hall coefficient was estimated at two typical fields of 1 kG (weak field) and 15 kG (strong field) using the following expression:

$$R_H = V_H d / IH \quad (1)$$

where V_H , I , H and d are the Hall voltage, current, applied field and thickness of the sample, respectively. The Hall coefficient at 1 kG is suitable for estimation of the carrier density and that at 15 kG (the strongest field used in the present study) is used to monitor non-linearity of the Hall voltage.

Figure 4 shows the Hall coefficient as a function of temperature at magnetic fields of 1 and 15 kG. In the high-temperature range ($T > 100$ K), the two curves of the Hall coefficient at 1 and 15 kG tend to merge into a single curve. This result indicates that, in

the high-temperature range, the Hall voltage is proportional to the magnetic field in the range $H < 15$ kG. The inset in figure 4 shows a linear dependence of the Hall voltage on the applied field at 77 and 290 K. On the other hand, below 100 K, the Hall voltage shows saturation and the Hall coefficient shows a different behaviour depending on the applied field. We note amongst other features that at $H = 1$ kG the Hall coefficient does change its sign at around 7 K. That is, the conduction below 7 K is electron like in contrast with the hole conduction in the high-temperature region.

4. Analysis and discussion

4.1. Three-carrier model

In order to explain the experimental results presented above, we assumed that three types of conduction are responsible for the transport phenomena at low temperatures in black-P crystals produced by the bismuth-flux method. These include

- (i) bulk hole conduction in the valence band,
- (ii) bulk conduction by the variable-range hopping (VRH) on acceptor levels, and
- (iii) 2D electron conduction in the surface layer.

The conductivity, mobility and hole concentration in the bulk hole conduction regime have been measured in the high-temperature range and discussed in detail in our previous paper [7]. The existence of 2D electron conduction has been confirmed by the analysis of negative magnetoresistances observed at low temperatures in black-P crystals obtained by the bismuth-flux method [8]. On the other hand, the VRH conduction has not yet been confirmed. The occurrence of VRH conduction, however, will be made clear in the following analysis.

In the measuring geometry shown in figure 1, where the electric field E is applied along the x axis and the magnetic field H is applied along the z axis, the average velocities v_i ($i = 1, 2, 3$) of the three types of carriers in a steady state are expressed as

$$v_i = \mu_i E + \mu_i v_i H/c \quad (2)$$

where μ_i is the mobility and c is the velocity of light in the vacuum. Hereafter, the subscripts 1, 2 and 3 refer to the bulk hole conduction, VRH conduction and 2D electron conduction, respectively. The total current along the x axis is given by

$$j_x = \sum_i n_i q_i v_{ix} \quad (3)$$

where n_i and q_i are the concentration and charge of each carrier. The total current along the y axis is given by

$$j_y = \sum_i n_i q_i v_{iy} = 0. \quad (4)$$

The y component in equation (2) is

$$v_{iy} = \mu_i E_y - \mu_i v_{ix} H/c. \quad (5)$$

Substituting equation (5) into equation (4), we have

$$E_y = \left(\sum_i n_i q_i \mu_i v_{ix} / \sum_i n_i q_i \mu_i \right) \frac{H}{c}. \quad (6)$$

Then, substituting equations (5) and (6) into the x component of equation (2), we have

$$v_{ix} = \mu_i E_x + \mu_i^2 \left(\frac{\sum_i n_i q_i \mu_i v_{ix}}{\sum_i n_i q_i \mu_i} - v_{ix} \right) \left(\frac{H}{c} \right)^2. \quad (7)$$

From equation (7) ($i = 1, 2, 3$), we have

$$\left[1 + \mu_1^2 \left(\frac{H}{c} \right)^2 - \left(n_1 q_1 \mu_1 / \sum_i n_i q_i \mu_i \right) \mu_1^2 \left(\frac{H}{c} \right)^2 \right] v_{1x} - \left(n_2 q_2 \mu_2 / \sum_i n_i q_i \mu_i \right) \times \mu_1^2 \left(\frac{H}{c} \right)^2 v_{2x} - \left(n_3 q_3 \mu_3 / \sum_i n_i q_i \mu_i \right) \mu_1^2 \left(\frac{H}{c} \right)^2 v_{3x} = \mu_1 E_x \quad (8)$$

$$- \left(n_1 q_1 \mu_1 / \sum_i n_i q_i \mu_i \right) \mu_2^2 \left(\frac{H}{c} \right)^2 v_{1x} + \left[1 + \mu_2^2 \left(\frac{H}{c} \right)^2 - \left(n_2 q_2 \mu_2 / \sum_i n_i q_i \mu_i \right) \times \mu_2^2 \left(\frac{H}{c} \right)^2 \right] v_{2x} - \left(n_3 q_3 \mu_3 / \sum_i n_i q_i \mu_i \right) \mu_2^2 \left(\frac{H}{c} \right)^2 v_{3x} = \mu_2 E_x \quad (9)$$

and

$$- \left(n_1 q_1 \mu_1 / \sum_i n_i q_i \mu_i \right) \mu_3^2 \left(\frac{H}{c} \right)^2 v_{1x} - \left(n_2 q_2 \mu_2 / \sum_i n_i q_i \mu_i \right) \mu_3^2 \left(\frac{H}{c} \right)^2 v_{2x} + \left[1 + \mu_3^2 \left(\frac{H}{c} \right)^2 - \left(n_3 q_3 \mu_3 / \sum_i n_i q_i \mu_i \right) \mu_3^2 \left(\frac{H}{c} \right)^2 \right] v_{3x} = \mu_3 E_x. \quad (10)$$

Solving the above simultaneous equation (equations (8)–(10)), we can obtain

$$R_H = \left(\frac{H}{c} \right) \left(\frac{\sum_i n_i q_i \mu_i \frac{\mu_i}{1 + \mu_i^2 (H/c)^2}}{\sum_i n_i q_i \mu_i \frac{1}{1 + \mu_i^2 (H/c)^2}} \right) \times \left(\frac{\sum_i n_i q_i \mu_i \frac{1 + \mu_i (E_y/E_x) (H/c)}{1 + \mu_i^2 (H/c)^2}}{\sum_i n_i q_i \mu_i \frac{1}{1 + \mu_i^2 (H/c)^2}} \right)^{-1} \quad (11)$$

where

$$\frac{E_y}{E_x} = \frac{\sum_i n_i q_i \mu_i \frac{\mu_i (H/c)}{1 + \mu_i^2 (H/c)^2}}{\sum_i n_i q_i \mu_i \frac{1}{1 + \mu_i^2 (H/c)^2}}. \quad (12)$$

If the magnetic field is weak, equation (11) can be reduced to

$$R_H = \frac{1}{c} \frac{\sum_i n_i q_i \mu_i^2}{\left(\sum_i n_i q_i \mu_i \right)^2}. \quad (13)$$

The physical parameters such as carrier concentrations and mobilities used in the three-carrier model are discussed below.

4.1.1. Bulk hole conduction. From the experimental results of the electric conductivity and the Hall coefficient below about 50 K, the concentration n_1 of the holes is approximately given by the equation

$$n_1 = 1 \times 10^{22} \exp(-137/T) \text{ m}^{-3} \quad (14)$$

with the activation energy of 137 K (11.8 meV) from the shallower acceptor level which

is dominant below 50 K [10]. The mobility μ_1 of the holes is assumed to be expressed as $1/\mu_1 = 1/\mu_{\text{ph}} + 1/\mu_{\text{imp}}$. Here, μ_{ph} is the mobility due to the acoustic phonon scattering and has been found to be proportional to $T^{-3/2}$ [4, 7] and μ_{imp} , the mobility due to the impurity scattering, is assumed to be nearly constant. Therefore, μ_1 is given by the equation

$$\mu_1 = A/(T^{3/2} + B) \text{ m}^2 \text{ V}^{-1} \text{ s}^{-1} \quad (15)$$

where the numerical parameters A and B are determined so as to fit to the experimental curve of the mobility, conductivity and Hall coefficient.

4.1.2. VRH conduction between acceptor levels. A two-carrier model consisting only of the bulk holes and the 2D electrons can also explain the occurrence of the sign reversal of the Hall coefficient, but quantitative agreement between its prediction and experiment is quite poor, which motivates the introduction of the third type of carrier, i.e. holes moving on acceptor levels by variable-range hopping. Assuming that the hopping hole concentration n_2 is almost constant and comparable with the acceptor concentration, we may consider that n_2 [7] and the mobility μ_2 [11] are given by

$$n_2 \approx 1 \times 10^{21} \text{ m}^{-3} \quad (16)$$

and

$$\mu_2 = \mu_0 \exp\{- (T_0/T)^{1/4}\} \text{ m}^2 \text{ V}^{-1} \text{ s}^{-1}. \quad (17)$$

Here, the numerical parameters μ_0 and T_0 in μ_2 are determined by fitting to the experimental conductivity σ and Hall coefficient R_{H} .

4.1.3. 2D electron conduction. The thickness d of the present sample was determined to be $6.5 \times 10^{-6} \text{ m}$ by SEM observation and the thickness t of the 2D layer near the surface to be $5 \times 10^{-8} \text{ m}$ by analysis [6] of the observed magnetoresistance based on the 2D localization theory [9].

According to the 2D localization theory, the sheet conductivity σ_{\square} is given by

$$\sigma_{\square}(T) = \sigma_{\square 0} + (e^2/2\pi^2\hbar) \times 10^{-5} \log TS \quad (18)$$

where

$$e^2/2\pi^2\hbar = 1.23 \times 10^{-5} \text{ S}. \quad (19)$$

An apparent conductivity σ_3 at a temperature below about 7 K is given approximately by

$$\sigma_3(T) = \sigma_{\square}(T)/d = en_3\mu_3 \text{ S m}^{-1} \quad (20)$$

where the second equality defines the apparent electron concentration n_3 and the electron mobility μ_3 . n_3 was determined to be $5 \times 10^{21} \text{ m}^{-3}$ from the value of R_{H} in the low-temperature region (figure 4). If the value of n_3 is assumed to be independent of the temperature, the mobility μ_3 is obtained from equations (18) and (20) as

$$\mu_3 = (2 \times 10^{-5} + 1.23 \times 10^{-5} \log T)/5.2 \times 10^{-3} \text{ m}^2 \text{ V}^{-1} \text{ s}^{-1}. \quad (21)$$

The mobility μ_3 can also be estimated using the surface electron concentration $n_{2\text{D}}$

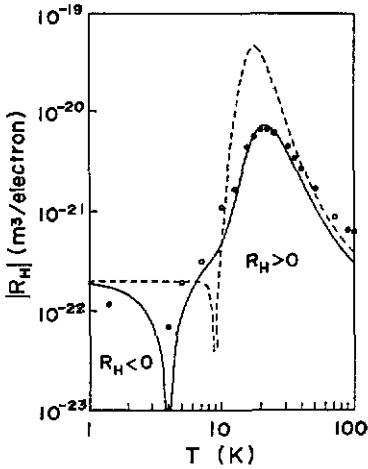


Figure 5. Absolute values of calculated and experimental Hall coefficients as a function of temperature at 1 kG: —, three-carrier model (using equation (13) in the text); - - -, two-carrier model.

in the 2D layer. It is related to the Fermi energy ε_F and the diffusion coefficient D of the electron by

$$\mu_3 = (e/\varepsilon_F)D \quad (22)$$

where ε_F is defined by

$$\varepsilon_F = (\hbar^2/2m^*)\pi n_{2D}. \quad (23)$$

Here, the surface electron concentration n_{2D} is given by

$$n_{2D} = n_3 d \approx 3.3 \times 10^{16} \text{ m}^{-2}. \quad (24)$$

Using equations (23) and (24), the mean effective mass $m^* = 0.22 m_0$ [12], and the value of D which was given as $6 \times 10^{-4} \text{ m}^2 \text{ s}^{-1}$ elsewhere [6], we have $\mu_3 \approx 3.4 \times 10^{-2} \text{ m}^2 \text{ V}^{-1} \text{ s}^{-1}$. This value is the same order of magnitude as that given by equation (21), which is $0.9 \times 10^{-2} \text{ m}^2 \text{ V}^{-1} \text{ s}^{-1}$, say, at 10 K.

4.2. Temperature dependence

The Hall coefficient R_H was calculated using equation (13) in the low-field limit and was fitted to the experimental data by varying A and B in equation (15) and μ_0 and T_0 in equation (17). Figure 5 shows the comparison between the calculated (full curve) and experimental R_H at 1 kG. The values of the parameters used in the calculation are $A = 2400 \text{ K}^{3/2} \text{ m}^2 \text{ V}^{-1} \text{ s}^{-1}$, $B = 300 \text{ K}^{3/2}$, $T_0 = 13000 \text{ K}$ and $\mu_0 = 23 \text{ m}^2 \text{ V}^{-1} \text{ s}^{-1}$. The above value of A is larger by a factor of 8 than the experimental value [7]. The discrepancy may be partly due to experimental errors or a scattering of samples. The calculated R_H is in accordance with experiments, i.e. it reproduces the maximum at around 30 K, a shoulder near 10 K, and the inversion of the sign at about 7 K. As a trial for another possibility, we have also calculated the Hall coefficient using a two-carrier model consisting only of the bulk holes and 2D electrons. The broken curve in the figure shows the R_H calculated by the two-carrier model, which was obtained by subtracting the VRH component from the R_H by the three-carrier model (full curve). The result is unreasonable, since the sign reversal is shifted from around 4 K to around 9 K and the value of R_H becomes much larger than the experimental results at around 20 K.

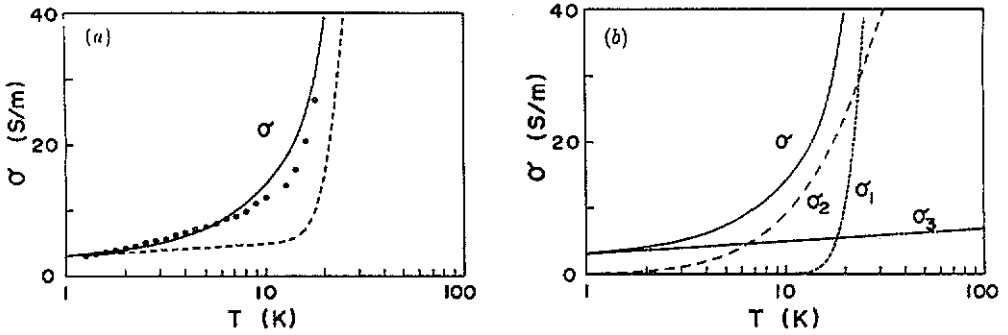


Figure 6. (a) Calculated (—) and experimental (O) conductivities as a function of temperature and (b) the total σ and three components σ_1 , σ_2 and σ_3 of calculated conductivity. The broken curve in (a) was calculated by the two-carrier model.

We have also calculated the conductivity using the same values of the parameters as those used in the calculation of R_H . Figure 6(a) shows the calculated (full curve) and experimental conductivity. The calculated curve is in good accordance with experiment and reproduces the $\log T$ -like dependence of σ . The broken curve shows the conductivity calculated by the two-carrier model. The result indicates that the two-carrier model cannot be fitted to the experimental data. Figure 6(b) shows σ_1 , σ_2 , σ_3 and $\sigma = \sigma_1 + \sigma_2 + \sigma_3$, where σ_1 is the conductivity due to the bulk hole conduction, σ_2 that due to the VRH conduction and σ_3 that due to the 2D electron conduction. We find that the 2D conduction is dominant at low temperatures below 7 K and the VRH conduction puts in an appearance only in a rather narrow temperature range around 10 K.

We note that, in the present successful analysis, only the numerical values obtained by experiments [7] and the universal constants from the 2D Anderson localization theory [9] were used except those of the VRH conduction. The characteristic temperature T_0 of the VRH conduction, which was one of the fitting parameters, was obtained to be 13 000 K. This value is much smaller than those for p-type InP [13], suggesting a large density of states and/or large localization length of holes in black P [14]. Further observations on the VRH conduction in black P are desirable in the present situation.

4.3. Magnetic field dependence

For large magnetic fields, the Hall coefficient R_H must be calculated using the original equation (11). Figure 7 shows the calculated and experimental R_H at 15 kG and their comparisons with those at 1 kG shown in figure 5. Above 10 K, the theoretical result at 15 kG is in fairly good agreement with experiments but *does change* its sign below about 7 K in contrast with the experimental data. The origin of this discrepancy between theory and experiment at high magnetic fields is not clear at present.

5. Conclusions

We have observed that black-P crystals prepared by the bismuth-flux method have the characteristic properties that the electric conductivity shows a $\log T$ -like behaviour below about 5 K and the Hall coefficient shows its sign reversal at around 7 K. We have

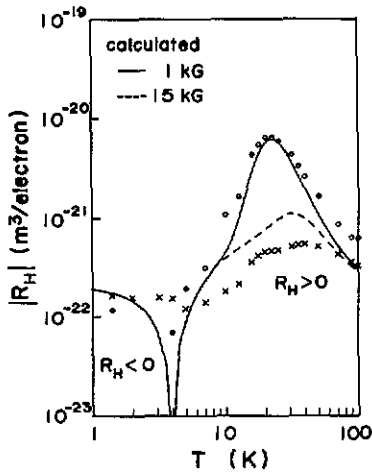


Figure 7. Calculated (---) and experimental (\times) Hall coefficients as a function of temperature at 15 kG, together with the corresponding Hall coefficients at 1 kG (\circ , observed points; —, calculation using equation (11) in the text) are also shown: \bullet , R_{H1} -values which are negative. The theoretical curve for $T < 7$ K is negative.

also found that these observations can be analysed successfully, except in the case of strong magnetic fields below 7 K, by the three-carrier model, in which bulk holes, VRH holes, and 2D electrons take part in the electric conduction at low temperatures. The two-carrier model without VRH holes cannot explain the experimental results. The success of the three-carrier model containing 2D electrons gives further support to the model that the negative magnetoresistance effect observed at low temperatures in the black-P crystal [6] originates from the Anderson localization of a 2D electron gas in the inversion surface layer.

The three-carrier model cannot explain the disappearance of the sign reversal of the Hall coefficient observed at strong magnetic fields. Its physical origin is not known and is left for future studies.

Acknowledgments

This work was performed under the Visiting Researcher's Program of the Institute for Materials Research, Tohoku University, and is supported in part by a Grant-in-Aid for Scientific Research from the Ministry of Education, Science and Culture, Japan.

References

- [1] Keys R W 1953 *Phys. Rev.* **92** 580–4
- [2] Warschauer D 1963 *J. Appl. Phys.* **34** 1853–60
- [3] Maruyama Y, Suzuki S, Kobayashi K and Tanuma S 1981 *Physica B* **105** 99–102
- [4] Akahama Y, Endo S and Narita S 1983 *J. Phys. Soc. Japan* **52** 2148–55
- [5] Iwasaka N, Maruyama Y, Kurihara S, Shirotani I and Kinoshita M 1985 *Chem. Lett.* 119–22
- [6] Baba M, Izumida F, Takeda Y, Shibata K, Morita A, Koike Y and Fukase T 1991 *J. Phys. Soc. Japan* **60** 3777–83
- [7] Baba M, Izumida F, Morita A, Koike Y and Fukase T 1991 *Japan. J. Appl. Phys.* **30** 1753–8
- [8] Baba M, Izumida F, Takeda Y and Morita A 1989 *Japan. J. Appl. Phys.* **28** 1019–22
- [9] Hikami S, Larkin A I and Nagaoka Y 1980 *Prog. Theor. Phys.* **63** 707–10
- [10] See figure 7 of [7]
- [11] Mott N F and Davis E A 1979 *Electronic Processes in Non-Crystalline Materials* (Oxford: Clarendon)

- [12] Narita S, Terada S, Mori S, Muro K, Akahama Y and Endo S 1983 *J. Phys. Soc. Japan* **52** 3544–53
- [13] Benzaquen M and Belache B 1990 *Phys. Rev. B* **41** 12 582–9
- [14] Mott N F 1969 *Phil. Mag.* **19** 835–52